

Assessment of ICESat performance at the salar de Uyuni, Bolivia

H. A. Fricker,¹ A. Borsa,¹ B. Minster,¹ C. Carabajal,² K. Quinn,³ and B. Bills⁴

Received 5 May 2005; revised 22 July 2005; accepted 27 July 2005; published 9 September 2005.

[1] The primary goal of the Ice, Cloud and land Elevation Satellite (ICESat) mission is ice sheet elevation change detection. Confirmation that ICESat is achieving its stated scientific requirement of detecting spatially-averaged changes as small as 1.5 cm/year requires continual assessment of ICESat-derived elevations throughout the mission. We use a GPS-derived digital elevation model (DEM) of the salar de Uyuni, Bolivia for this purpose. Using all twelve ICESat passes over the salar survey area acquired to date, we show that the accuracy of ICESat-derived elevations is impacted by environmental effects (e.g., forward scattering and surface reflectance) and instrument effects (e.g., pointing biases, detector saturation, and variations in transmitted laser energy). We estimate that under optimal conditions at the salar de Uyuni, ICESat-derived elevations have an absolute accuracy of <2 cm and precision of <3 cm. **Citation:** Fricker, H. A., A. Borsa, B. Minster, C. Carabajal, K. Quinn, and B. Bills (2005), Assessment of ICESat performance at the salar de Uyuni, Bolivia, *Geophys. Res. Lett.*, 32, L21S06, doi:10.1029/2005GL023423.

1. Introduction

[2] NASA's Geoscience Laser Altimeter System (GLAS) on the Ice, Cloud and land Elevation Satellite (ICESat) is Earth's first polar-orbiting satellite laser altimeter. ICESat's primary objective is to detect changes in ice sheet elevations of as little as 1.5 cm/year, spatially-averaged over 100 × 100 km [Zwally *et al.*, 2002]. This ambitious goal requires precise calibration and validation of the instrument throughout the ICESat mission. One approach for validating the ICESat-derived elevations is to compare them to an accurately-surveyed terrestrial reference target. Salt flats are ideal for this purpose since they are large, stable surfaces that are amenable to detailed surveying and have an albedo similar to that of ice sheets.

[3] We selected the largest salt flat in the world, the 9600 km² salar de Uyuni on the Bolivian Altiplano, as a reference target for the ICESat mission. The salar is a stable equipotential surface that is continually levelled and smoothed by seasonal flooding during the austral summer [Borsa, 2005]. We surveyed the salar's large eastern lobe

using kinematic GPS and constructed a DEM of the surface from this data (Figure 1).

[4] To date ICESat has overflown our survey area twelve times during six separate ICESat operations periods (Table 1). In this paper we compare ICESat elevations derived from the GLAS altimetry channel (1064 nm) with the salar de Uyuni DEM, showing how differing conditions between passes affect ICESat performance. We also quantify the absolute and relative accuracy of the ICESat elevations for each operations period. These results are crucial for understanding the capabilities and the limitations of the current ICESat datasets for ice sheet change detection.

2. GPS Survey and Data Processing

[5] We surveyed a 54 × 45 km section of the salar de Uyuni at the end of the dry season, on 3–8 September 2002. We divided this survey area into eight smaller grids, which we surveyed independently. Our survey vehicles each carried a dual-frequency Ashtech Z-12 receiver (at 3-s sampling) and a roof-mounted choke-ring antenna. We drove at an average speed of 120 km/h, providing 100 m along-track spacing between GPS measurements. Cross-track spacing was 2.25 km, which was sufficient to characterize the salar topography. We observed and maintained lock on at least seven satellites at all times. For ground control, we deployed three fixed GPS stations around each survey grid for 24-hour periods. We also operated a central GPS reference station over the entire 6-day survey period, whose WGS-84 elevation we established to 0.4 mm.

[6] Our GPS processing strategy is described extensively by Borsa [2005]. We determined fixed site positions by post-processing relative to the GPS reference station, using double-differences, the ionosphere-free LC combination, precise ephemerides and tropospheric delay correction. We estimated the fixed site elevation bias to be under 0.2 mm in all cases. For the kinematic data, which we processed relative to the fixed GPS stations, we additionally estimated GPS noise due to multipath and the troposphere using an algorithm we developed for the salar survey. After removing this noise, we constructed a DEM of the surface (the "salar DEM," Figure 1). Total elevation range over the DEM is only 0.78 m, with a broad surface slope from northeast to southwest that approximately mimics the long-wavelength EGM-96 geoid. Based on various consistency checks and comparisons with independent GPS data, we estimate that the DEM has local biases of no more than 1 cm over the entire survey area.

3. ICESat Data Analysis

[7] Since 4 October 2003, ICESat has been operating in a 91-day exact repeat orbit, with 30-km cross-track spacing at the equator (B. Schutz *et al.*, ICESat Mission overview, submitted to *Geophysical Research Letters*, 2005, hereinaf-

¹Institute of Geophysics and Planetary Physics, Scripps Institution of Oceanography, La Jolla, California, USA.

²NVI, Inc., Greenbelt, Maryland, USA.

³Jet Propulsion Laboratory, California Institute of Technology, Pasadena, California, USA.

⁴NASA Goddard Space Flight Center, Planetary Geodynamics Laboratory, Greenbelt, Maryland, USA.

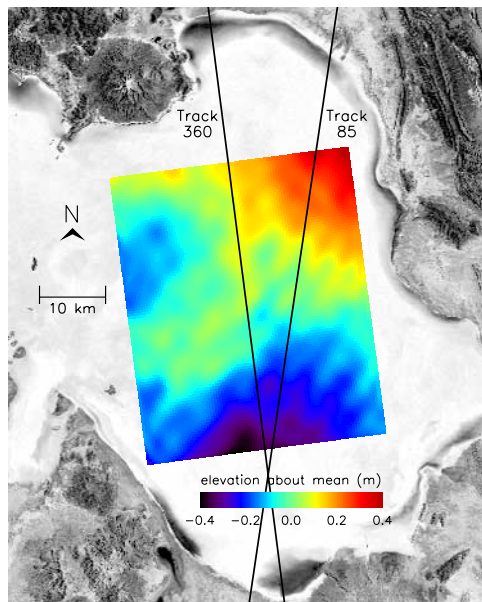


Figure 1. Landsat ETM image of salar de Uyuni showing the DEM generated from our GPS survey. The two 91-day ICESat ground tracks (0085 and 0360) are overlaid.

ter referred to as Schutz et al., submitted manuscript, 2005). The six ICESat operations periods we discuss took place during approximately the same 33-day sub-cycle of this 91-day orbit, with Tracks 85 (descending) and 360 (ascending) crossing our survey area (Figure 1).

[8] At the time of writing, ICESat data from each operations period are still in different post-processing states, as expressed by the data release number in Table 1. The main difference between releases is the successive refinement of instrument pointing biases (see *Luthcke et al.*, 2005). We note that over an area the size of the salar, which ICESat overflies in seconds, pointing biases generally manifest themselves as elevation biases. We used the latest available releases for each operations period, noting that efforts by the ICESat Science Team are ultimately expected

to bring all data to 2 arcsec pointing accuracy (Schutz et al., submitted manuscript, 2005).

[9] We obtained geolocated laser footprint locations from the GLA06 Global Elevation Data Product. For each footprint, we also obtained a record of the echo waveform, transmitted and received laser energy and receiver gain from the GLA01 Global Altimetry Data Product. Since ICESat coordinates are referenced to the TOPEX ellipsoid, we converted footprint locations to WGS-84 ellipsoidal coordinates for comparison with GPS data. We then obtained the GPS “reference elevation” by interpolating the salar DEM to the locations of the laser footprints.

4. Results and Discussion

[10] For all twelve ICESat passes over the salar survey area, we determined the accuracy of the ICESat-derived elevations by comparing them with their reference elevations. The results are summarized in Table 1, where the last column shows the mean and standard deviation (SD) of the difference between ICESat-derived elevations and the GPS reference elevations. Hereafter, we refer to the mean of the difference as the “elevation bias.”

[11] ICESat performance is compromised by detector saturation from high pulse return energy, forward scattering from clouds, and higher noise when the transmitted laser power declines. Similar effects have been observed in ICESat data collected over the ice sheets.

4.1. Detector Saturation (Laser 2a, Track 085)

[12] Laser 2a Track 85 was acquired during clear atmospheric conditions. For the GLAS 1064 nm altimeter channel, high laser return energy combined with the inability of the automatic gain control to adjust below its present lower limit causes detector saturation: high return energy overloads the detector, leading to distorted waveforms that are clipped and artificially wide [*Sun et al.*, 2003]. For such waveforms, ICESat’s standard Gaussian fit processing is biased toward longer ranges, leading to low elevation estimates (J. Abshire et al., ICESat: GLAS on orbit science measurements through March 2005, submitted to *Geophys-*

Table 1. Operating Periods, Data Release Number, Dates, Environmental Conditions, Average Transmitted and Return 1064 nm Energy, Number of ICESat Points (N) and Difference Statistics (ICESat Minus GPS DEM Elevations) for Twelve ICESat Passes Acquired Over salar de Uyuni Survey Area

Ops Period	Data Release	Track	Date	Cloud Cover	Surface Water	Transmit Energy, mJ	Return Energy, fJ	Number of Points	Mean Difference ± Standard Deviation, cm
Laser 2a	21	085	10-27-2003	None	None	71	19.5	320	-9.6 ± 4.9^a , -1.9 ± 3.2^b
Laser 2a	21	360	11-14-2003	Heavy	None	63	0.9	154	-16.0 ± 7.9
Laser 2b	16	085	02-28-2004	Minimal	Minimal	46	10.2	320	0.5 ± 3.2
Laser 2b	16	360	03-17-2004	Minimal	Minimal	38	8.2	307	1.2 ± 2.7
Laser 2c	17	085	05-29-2004	None	None	15	3.7	320	33.0 ± 4.8
Laser 2c	17	360	06-16-2004	Minimal	None	7	1.9	308	23.5 ± 8.3
Laser 3a	22	085	10-14-2004	None	None	60	15.5	321	-16.9 ± 3.9^a , -13.6 ± 2.8^b
Laser 3a	22	360	11-01-2004	Variable	None	66	10.6	308	-12.0 ± 4.6^a , -11.1 ± 3.9^b
Laser 3b	19	085	03-02-2005	None	Present	62	84.5	319	-102.5 ± 3.7
Laser 3b	19	360	03-20-2005	None	Variable	54	50.3	308	-85.0 ± 53.4
Laser 3c	22	085	05-31-2005	None	None	53	13.5	321	18.2 ± 4.1
Laser 3c	22	360	06-19-2005	None	None	49	13.7	309	-42.4 ± 3.2

Transmit energy is corrected by a factor of 1.129 for Laser 2 and 1.121 for Laser 3 (X. Sun, personal communication, 2005).

^aStandard geolocation.

^bSaturation correction applied.

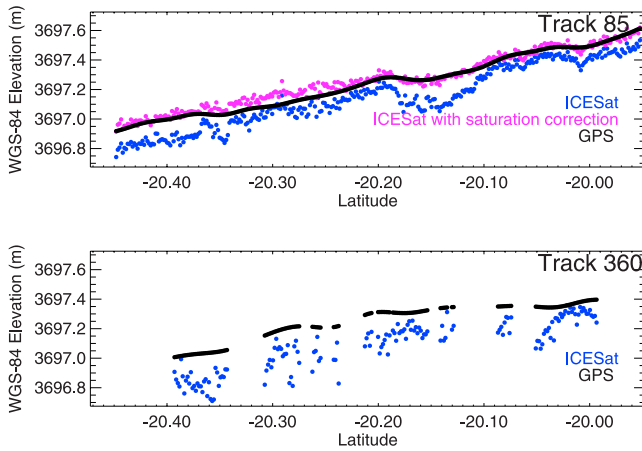


Figure 2. Comparison of ICESat Laser 2a elevations with their reference GPS elevations. (Top) Track 85, raw elevations (blue), saturation-corrected elevations (magenta). (Bottom) Track 360, with no saturation correction needed because of low return energy induced by clouds. Noise in Track 360 is due to forward scattering.

ical Research Letters, 2005, hereinafter referred to as Abshire et al., submitted manuscript, 2005).

[13] Figure 2 (top) compares ICESat-derived elevations from Track 85 (blue) with the salar DEM (black). ICESat elevations deviate from the true surface, especially in the shallow topographic depression around latitude 20.15°S where the waveforms are most saturated. Investigation of the saturation effect by the GLAS instrument team resulted in an empirical correction for the two-way travel time of all pulses whose return energy (E) calculated from the pulse area is greater than a threshold value (E_{sat}) [Sun et al., 2003]. The time-of-flight correction to be subtracted from the reported value is $\delta t = \alpha(E - E_{sat})$, $E > E_{sat}$, where α is a linear scale factor. This formula is valid only when the detector gain is at the lowest gain setting of 13 (i.e., “low-gain saturation”). Laboratory tests give $\alpha = 0.149$ ns/fJ and $E_{sat} = 13.1$ fJ (X. Sun, personal communication, 2005). This implies a saturation range bias of 15 cm at 20 fJ, which is significant considering the ICESat mission accuracy requirement. Since in all releases to date the reported waveform energy in GLA01 is incorrect, we recalculate it from the echo waveforms using:

$$E = \frac{0.1165}{\text{gain}} \sum_i (w_i - \varepsilon)$$

where ε is the mean background noise for the waveform, w_i is the waveform count at bin i , $\text{gain} = 13$, and energy is in fJ (X. Sun, personal communication, 2005).

[14] We show the results of applying the laboratory-derived saturation correction to Track 85 in Figure 2 (top) (blue). The correction improved the fit to the salar DEM significantly, reducing the elevation bias from -9.6 cm to -1.9 cm and the SD from 4.9 cm to 3.2 cm (Table 1). This result indicates that the laboratory saturation formula models the saturation effect accurately (at least at these return energies). Significantly, we note that return energies

over Uyuni for this pass are similar in magnitude (19 fJ vs 26 fJ) to those from Lake Vostok, East Antarctica collected one day earlier (C. A. Shuman et al., *Ice Sheet Elevations from ICESat, 2003–2004*, submitted to *Geophysical Research Letters*, 2005). These energy levels are considerably above the saturation threshold and are typical of ice sheet echoes elsewhere during Laser 2a, underscoring the importance of the saturation correction for studies requiring sub-decimeter-level knowledge of ice sheet elevation.

4.2. Forward Scattering (Laser 2a, Track 360)

[15] Thick cirrus clouds were present during Laser 2a, Track 360, generally attenuating laser return energy. 13% of the GLAS pulses were unable to penetrate the cloud cover. ICESat performance under cloudy conditions is degraded by forward scattering of photons within the cloud layer, which delays their return to the detector and produces a long “tail” in the echo waveform. On this pass, the result is high noise (SD is 7.9 cm) and anomalously low elevation estimates (-16 cm bias), as illustrated in Figure 2 (bottom). Although instrument pointing biases may contribute to the elevation bias, the magnitude of the elevation bias and scatter in Track 360 relative to Laser 2a Track 80 indicates the presence of atmospheric forward scattering.

4.3. Nominal Laser Operation (Laser 2b)

[16] The results for Laser 2b demonstrate the low noise of the ICESat-derived elevations under ideal conditions. Both tracks were acquired under clear conditions and with nominal return energies (i.e., $E < E_{sat}$). The elevation SD for both tracks is 3 cm. Bias for both tracks is also low (~ 1 cm), although we reiterate that all data prior to Release 21 do not have complete pointing corrections applied [Lutcke et al., 2005] and we expect that the biases will change when these data are reprocessed.

4.4. Low Transmit Power (Laser 2c)

[17] Transmitted laser energy declined considerably from Laser 2b to Laser 2c (Table 1). Although on-board gain control compensates for lower-energy echo pulses, noise is amplified along with the signal. This degrades pulse timing accuracy, as the plot of return energy versus data misfit in Figure 3 shows. We conclude that the large elevation SD of Laser 2c Track 85 (4.8 cm) and Track 360 (8.6 cm) are the result of this effect.

4.5. Possible Pointing Errors (Laser 3a)

[18] Laser 3a, Track 085 over Uyuni was collected under clear conditions, with some echo waveforms showing saturation due to high return energy. The saturation correction reduced the elevation SD from 3.9 cm to 2.8 cm. The large elevation bias (-13.6 cm) is due to remaining pointing biases in Release 22 data (S. Lutcke, personal communication, 2005). For Track 360, cirrus clouds were present at approximately 10 km altitude (S. Palm, personal communication, 2005). Nevertheless, some waveforms were saturated, and the saturation correction reduced the SD from 4.6 cm to 3.9 cm. The slightly higher SD compared to Track 85 is due to forward scattering. Quantification of the forward scattering bias in this case is not possible until all pointing errors are minimized.

4.6. Extreme Detector Saturation (Laser 3b)

[19] Both Laser 3b passes occurred in March 2005, while the salar was flooded. Satellite images of the salar from 2 March show that Track 85 encountered a uniform layer of surface water. Specular echoes from the beam-normal face of small surface ripples may be responsible for the extremely high return energies observed (70–90 fJ). Although shot-to-shot noise (and thus SD) is low, at these energy levels the echo waveforms are heavily distorted, introducing a ~ 1 m bias in ICESat-derived elevations. Similar waveforms have been noted in the Florida Everglades (D. Harding, personal communication, 2005) and over leads in Arctic sea-ice (S. Farrell, personal communication, 2005). The saturation correction we use for Laser 2a does not work well for energies above 60 fJ, although an extended saturation correction model is currently being investigated.

[20] By the time Track 360 was acquired 18 days later, the salar surface had started to dry in some areas. The plot of Track 360 return energies, elevations and waveforms in Figure 4 illustrates how unsaturated, partially-saturated and super-saturated echo waveforms affect the ICESat-derived elevations. Although the bias and SD statistics of the track as a whole are poor (Table 1), unsaturated pulses align closely with the salar DEM, while increasing saturation levels result in increasingly poor elevation estimates.

5. Conclusions

[21] The salar de Uyuni is an excellent proxy for the central areas of the polar ice sheets, both in terms of albedo and flatness. The results from our comparisons of ICESat elevations with our GPS-derived DEM on the salar have

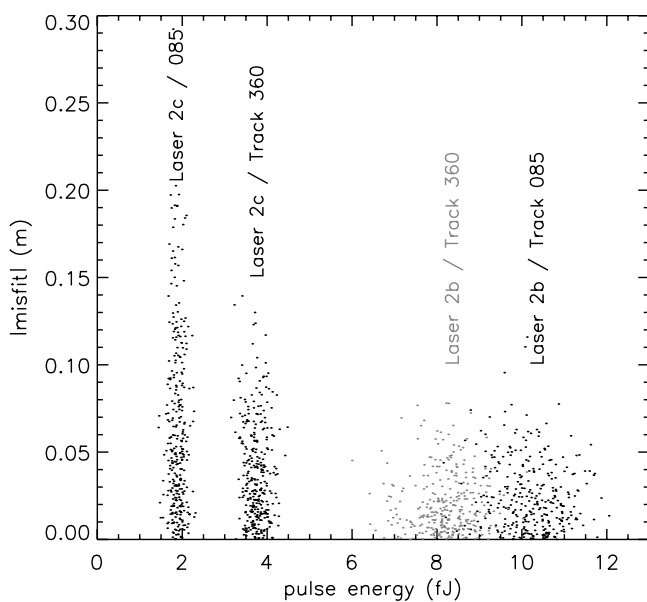


Figure 3. Correlation between elevation misfit and corrected return energy. Here, we define misfit as the absolute value of the difference between ICESat and GPS elevations, with mean difference removed. Decreasing transmitted laser power from Laser 2b to Laser 2c leads to increased noise in the ICESat-derived elevations.

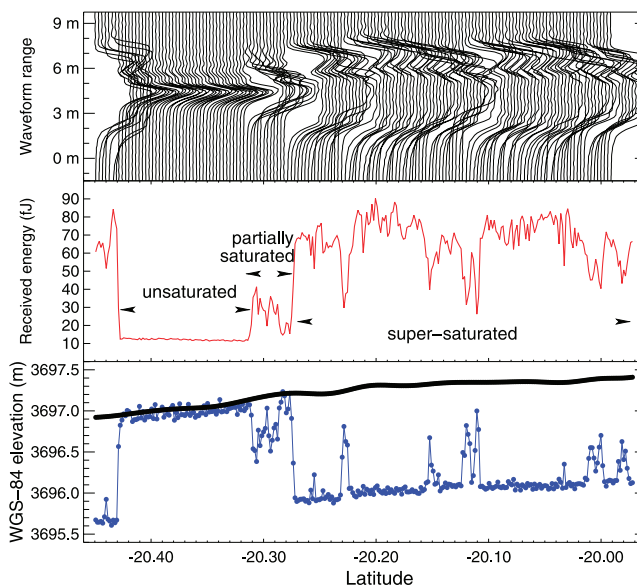


Figure 4. Laser 3b Track 360, acquired while the salar was partially flooded. (Top) waveform stack; (Middle) laser return energy; (Bottom) ICESat versus GPS elevations. Note the anti-correlation of elevation with return energy, which is the expected effect from saturation (Abshire et al., submitted manuscript, 2005).

important implications for ice sheet elevation change detection. Under ideal conditions with all pointing corrections applied (Laser 2a, Release 21 data), ICESat-derived elevations have an absolute accuracy (bias) of <2 cm and precision (SD) of <3 cm over the salar. However, we observe that ICESat performance degrades substantially under certain conditions. Atmospheric forward scattering results in increased measurement noise and a negative elevation bias, as expected. Degradation of the laser transmit power over time causes a noticeable increase in measurement noise when the echo pulse energy drops below about 5 fJ, which affects both the accuracy and precision of the elevations. Finally, detector saturation is a common problem that cannot be ignored at the accuracy level required for ice sheet change detection. Using our results, we have verified a laboratory-derived saturation correction that will be incorporated into future releases of ICESat data.

[22] The change in the ICESat elevation bias between the six ICESat operations periods and, to a lesser extent, between passes within the operations periods demonstrates the current limitations of geolocation values given in the latest releases of the ICESat products. Efforts underway by the ICESat Science Team to resolve pointing errors to the same level as that achieved for Laser 2a should remove much of this variability in the elevation bias [Luthcke et al., 2005]. As part of the ongoing calibration effort, we will continue to use the salar de Uyuni to assess and improve the accuracy of future data releases.

[23] **Acknowledgments.** We thank NASA's ICESat Science Project and the NSIDC for distribution of the ICESat data, see <http://icesat.gsfc.nasa.gov> and <http://nsidc.org/data/icesat>. Thanks to X. Sun, B. Schutz, S. Luthcke, and S. Palm for their helpful contributions. Uyuni fieldwork

and work at SIO funded through NASA contract NAS5-99006 to ICESat Team Member B. Minster. Comments of two anonymous reviewers are gratefully appreciated.

References

- Borsa, A. (2005), Geomorphology of the salar de Uyuni, Bolivia, Ph.D. thesis, Scripps Inst. Oceanogr., Univ. of Calif., San Diego, La Jolla.
- Luthcke, S. B., D. D. Rowlands, T. A. Williams, and M. Sirota (2005), Reduction of ICESat systematic geolocation errors and the impact on ice sheet elevation change detection, *Geophys. Res. Lett.*, doi:10.1029/2005GL023689, in press.
- Sun, X., J. B. Abshire, and D. Yi (2003), GLAS—Characteristics and performance of the altimeter receiver, *Eos Trans. AGU*, 84(46), Fall Meet. Suppl., Abstract C32A-0432.
- Zwally, J., et al. (2002), ICESat's laser measurements of polar ice, atmosphere, ocean, and land, *J. Geodyn.*, 34, 405–445.
-
- B. Bills, NASA Goddard Space Flight Center, Planetary Geodynamics Laboratory, Code 698, Greenbelt, MD 20771, USA.
- A. Borsa, H. A. Fricker, and B. Minster, IGPP, Scripps Institution of Oceanography, University of California, San Diego, 9500 Gilman Drive, La Jolla, CA 92093, USA. (hafricker@ucsd.edu)
- C. Carabajal, NVI, Inc., NASA Goddard Space Flight Center, Space Geodesy Laboratory, Code 697, Greenbelt, MD 20771, USA.
- K. Quinn, Jet Propulsion Laboratory, Caltech, Mail stop 238-332, Pasadena, CA 91109, USA.